Far-Infrared Energy Gap Measurements in Bulk Superconducting In, Sn, Hg, Ta, V, Pb, and Nb†

P. L. RICHARDS* AND M. TINKHAM
Department of Physics, University of California, Berkeley, California
(Received February 17, 1960)

Measurements of the onset of absorption due to excitation of electrons across the energy gap were made on a variety of superconductors. Using the onset of the main absorption edge as a measure of the energy gap, the values of $E_g(0)$, the energy gap at absolute zero, were found to be $4.1\pm0.2\ kT_c$ for indium, $3.6\pm0.2\ kT_c$ for tin, $4.6\pm0.2\ kT_c$ for mercury, $\leqq3.0\ kT_c$ for tantalum, $3.4\pm0.2\ kT_c$ for vanadium, $4.1\pm0.2\ kT_c$ for lead, and $2.8\pm0.3\ kT_c$ for niobium. The deviations of these values of the energy gap from the Bardeen-Cooper-Schrieffer value of $3.5\ kT_c$ are a fairly smooth function of the Debye temperature alone, but a less smooth one of the ratio of the Debye temperature to the critical temperature. Structure was found on the absorption curves of lead and mercury. Its interpretation is discussed in terms of possible states in the gap, anisotropy of the gap, and of a possible dielectric anomaly. The position of the main absorption edge seemed to scale with temperature according to the temperature dependence of the energy gap predicted by the Bardeen-Cooper-Schrieffer theory, and the structure appeared to have a roughly similar temperature dependence. The absorption curves for pure superconductors are compared with predictions based on the theory of the skin effect in the normal and superconducting states. Two alloy superconductors were measured. They appeared to have less well-defined gaps than the pure superconductors.

I. INTRODUCTION

IN the theory of superconductivity of Bardeen, Cooper, and Schrieffer[1] (BCS), a minimum energy of $E_g(0)=3.5\ kT_c$ is required to produce an excitation from the ground state, where T_c is the critical temperature. This minimum excitation energy, or energy gap, is a central result of the theory, and is sufficient to explain most of the electromagnetic and thermal properties of superconductors.[2,3]

Experimental evidence for the existence of the energy gap can be obtained from specific heat, thermal conductivity, nuclear relaxation, ultrasonic attenuation, and electromagnetic absorption data.[2] Unfortunately, most of these data require an interpretation in terms of a detailed theory before a value of the energy gap can be deduced.

Probably the most direct method of measuring the superconducting energy gap is by observing the onset of electromagnetic absorption in a bulk sample. This occurs when the incident electromagnetic quantum energy becomes large enough to excite electrons across the energy gap. At finite temperatures, this characteristic quantum absorption is superimposed on absorption caused by "normal" electrons that have been thermally excited across the gap to states from which arbitrarily small additional increases in energy are possible. The BCS theory predicts that the energy gap closes as the temperature approaches T_c, as is indicated by the absence of any latent heat in the field-free superconducting transition. Thus, at $T>0$, absorption due to excitations across the energy gap will occur at quantum energies less than $E_g(0)$. A number of investigators have observed this energy gap contribution to the microwave surface resistance[4] in the superconducting state close to the critical temperature[5] where the gap is small, and correspondingly many normal electrons are present.

In order to measure the width of the energy gap at the absolute zero, which is of most fundamental interest, one must be able to measure the surface resistance of the superconductor at temperatures much lower than T_c. Two general approaches have been used on this problem. One is to observe the onset of heating in a superconductor that is exposed to millimeter microwave radiation with $\hbar\omega\cong E_g(0)$. Present practical limitations on microwave quantum energies restrict this method to superconductors with low critical temperatures. This approach has been used on aluminum (for which $T_c=1.2°K$) by Biondi and Garfunkel,[6] who obtained temperatures of $\sim0.3\ T_c$ by the use of a liquid He^3 refrigerator. Their curves of R_S/R_N, the ratio of the surface resistances in the superconducting and normal states, extend to high enough quantum energies to show the onset of absorption at absolute zero due to bridging the energy gap. In this way Biondi and Garfunkel obtained the value $E_g(0)=3.2$

† Supported in part by the National Science Foundation, the Alfred P. Sloan Foundation, and the Office of Naval Research.
* National Science Foundation Predoctoral Fellow, now at the Royal Society Mond Laboratory, Cambridge, England.
[1] J. Bardeen, L. N. Cooper, and J. R. Schrieffer, Phys. Rev. **108**, 1175 (1957).
[2] M. A. Biondi, A. T. Forrester, M. P. Garfunkel, and C. B. Satterthwaite, Revs. Modern Phys. **30**, 1109 (1958).
[3] M. Tinkham and R. A. Ferrell, Phys. Rev. Letters **2**, 331 (1959).
[4] The surface resistance is the real part of the surface impedance Z, defined as $Z=(4\pi/c)(E/H)_0$, where $(E/H)_0$ is the ratio of electric to magnetic fields at the surface of the metal. In general, $Z=R+iX$ is complex; the imaginary part is the surface reactance. The microwave surface resistance R is directly related to the quality factor Q of a cavity and so can be measured relatively easily. The absorptivity $\mathfrak{a}$ of a metal surface is simply $\mathfrak{a}=cR/\pi$ so long as $\mathfrak{a}\ll1$, which is true for metals under most circumstances.
[5] See, for example, M. A. Biondi, M. P. Garfunkel, and A. O. McCoubrey, Phys. Rev. **108**, 495 (1957); and M. A. Biondi, A. T. Forrester, and M. P. Garfunkel, Phys. Rev. **108**, 497 (1957).
[6] M. A. Biondi and M. P. Garfunkel, Phys. Rev. Letters **2**, 143 (1959).

$\pm 0.1\ kT_c$ for the width of the energy gap in aluminum at absolute zero.

The other approach (followed in the research reported here) is to use superconductors such as indium, tin, mercury, tantalum, vanadium, lead, and niobium, with critical temperatures in the range from 3.3 to 9°K, for which temperatures much less than T_c can be reached with ordinary liquid He^4 techniques. For these superconductors, the wavelength range from 0.1 to 2 mm available from a far-infrared monochromator spans the transition from the essentially lossless behavior characteristic of superconductors at low frequencies to high-frequency absorption which, like that observed in the near-infrared,[7] is indistinguishable from that of the normal-state metal. It is not feasible, at present, to observe the heating of the sample due to the far-infrared radiation because the necessary power is not available. The approach used for bulk samples is to measure the difference between the power reflected from the sample when it is in the superconducting and normal states. The first measurements of this sort were reported by Richards and Tinkham on tin and lead.[8] The present paper contains a full report of our application of far-infrared techniques to the measurement of the energy gaps of bulk superconductors.

This research is also related to measurements of the transmission of far-infrared radiation through thin superconducting films, first made by Glover and Tinkham,[9] and recently improved by Ginsberg and Tinkham.[10] The film transmission data, when analyzed to separate the reflection from the absorption, give information about the onset of absorption due to the energy gap. The film experiments have almost an order of magnitude larger signal-to-noise ratio than the measurements on bulk samples because of the more favorable geometry and the large absorption in the normal film, but the interpretation in terms of an energy gap is less direct. In what follows, comparisons will be made between the two types of far-infrared experiments, where appropriate.

II. APPARATUS

Our experiment was performed by conveying the output of a far-infrared grating monochromator down a brass light pipe into an oversize, nonresonant, superconducting cavity immersed in liquid helium at various temperatures below T_c. The radiation made many reflections in the cavity to build up the metallic absorption to a measurable amount; a fraction was then absorbed in a carbon resistance bolometer mounted on the cavity wall. The power P_S that reached the bolometer when the cavity was in the superconducting state was compared to that P_N when the superconductivity was destroyed by the application of a magnetic field. Values of the fractional change $(P_S-P_N)/P_N$ in bolometer signal as the magnet was turned on and off were measured at various wavelengths in the range from 0.1 to 2 mm for a number of superconductors. These data give a measure of the difference between the reflectivities of the superconducting and normal states in the region of the energy gap.

A. Far-Infrared Monochromator

Among the best available sources for these far-infrared experiments is an ordinary G.E. type UA-3 quartz mercury arc lamp, which emits 360 watts of radiation, mostly in the ultraviolet, visible, and near infrared. Only $\sim 10^{-7}$ watt is, however, emitted in a 10% bandwidth at 0.5 mm. The rather severe problem of obtaining a rejection factor of over 10^9 for unwanted short-wavelength radiation was solved by a series of transmission filters and by the $f/1.5$ grating monochromator shown in Fig. 1. This monochromator was especially designed by D. M. Ginsberg and the authors to provide for the use of pairs of 3×4-inch echelette gratings in zero order as low-pass filters which systematically scatter the shorter wavelengths from the beam. At frequencies where the other filters are adequate, these gratings are replaced by plane mirrors. After emerging from the lamp, the radiation was focused by a spherical mirror onto the first zero-order grating. After reflecting off this grating, the light passed through a polyethylene filter, blackened with turpentine soot, which covered a hole in an opaque baffle. The baffle and filter prevented stray light from the lamp from being interrupted by the 9 cps light chopper and re-entering the optical path. A second spherical mirror brought the light leaving the second filter grating to a focus at a point near the output light pipe. The remainder of the optical system was an on-axis grating monochromator similar to the one used by McCubbin and Sinton.[11] That is, after the focus, the light diverged to a 12-inch diameter spherical collimating mirror with an 18-inch focal length, was reflected back to a 12-inch square echelette grating used in first order to provide the dispersion, and was refocused on the output light pipe by the collimating mirror.

Wavelengths were determined by measuring the angle of the 12-inch grating from the position of the zero-order spectrum. Coarse gratings with low dispersion were used, and there were no slits other than the source and the light pipe, so that radiation in a band width of $\sim 10\%$ was utilized. Dispersion gratings were used only near their blaze wavelength for maximum grating efficiency. The various echelette gratings were ruled on

[7] J. G. Daunt, T. C. Keely, and K. Mendelssohn, Phil. Mag. **23**, 264 (1937); K. G. Ramanathan, Proc. Phys. Soc. (London) **A65**, 532 (1952).

[8] P. L. Richards and M. Tinkham, Phys. Rev. Letters **1**, 318 (1958).

[9] R. E. Glover, III, and M. Tinkham, Phys. Rev. **108**, 243 (1957).

[10] D. M. Ginsberg and M. Tinkham, Phys. Rev. **118**, 990 (1960).

[11] T. K. McCubbin, Jr., and W. M. Sinton, J. Opt. Soc. Am. **42**, 113 (1952).

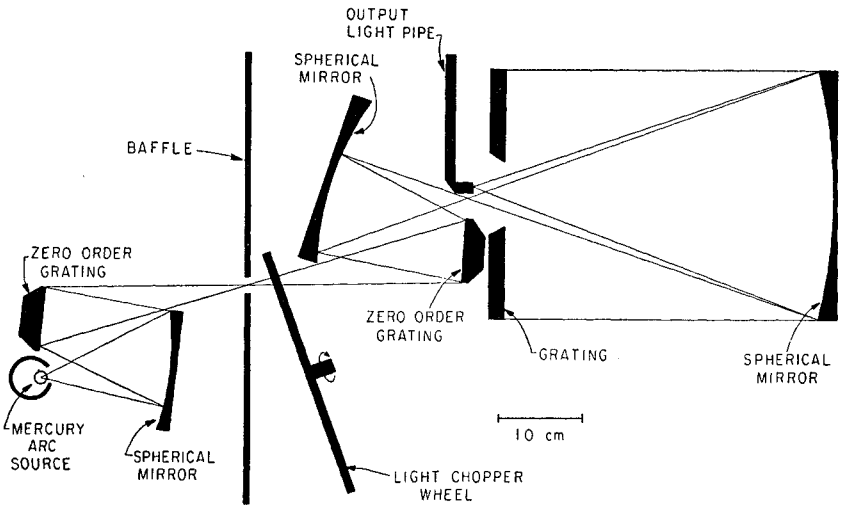

FIG. 1. Plan of far-infrared grating monochromator.

a planer, and had from 8 to 70 rulings per inch.[12] The mirrors were turned from solid dural and polished on a lathe. The end of the light pipe was fitted permanently with sooted polyethylene and crystal quartz filters, which were used at all wavelengths. Provision was made for attaching fused quartz and rock salt filters as needed[12] to suppress the second and higher orders of diffraction from the 12-inch grating.

The problem of focusing the $f/1.5$ radiation from the monochromator into a cavity cooled with liquid helium and placed in a magnet gap was solved by the use of a brass light pipe. An analysis of the use of metal light pipes in the far infrared has been separately published.[13] In this experiment about 4 feet of light pipe made from 0.43-inch i.d. brass tubing and giving a transmission of $\sim 70\%$ at 0.5-mm wavelength was used. This diameter corresponded to the 0.5-inch diameter of the mercury arc which was the effective input slit of the monochromator. The portion of the light pipe that was in the Dewar was turned down to a 0.010-inch wall thickness to minimize the conductive heat leak along the pipe into the liquid helium. Two right-angle bends of the type described in reference 12 were needed to convey the horizontal beam of radiation from the monochromator into the vertical Dewar.

B. Analysis of Cavity Response

Since the radiation from the monochromator was relatively broad band and had wavelengths short compared to typical cavity dimensions, the response of the cavity consisted of a large number of closely spaced resonant modes that were nearly equally excited. Thus we can describe the radiation in the cavity in terms of a uniform distribution of photons as discussed by Lamb.[14] Using his expressions for the quality factor Q, we may deduce the response of a cavity consisting of a coupling hole of area A_H and associated $Q_H=8\pi V/\lambda A_H$, a bolometer with an effective black area A_B with $Q_B=8\pi V/\lambda A_B$, and cavity walls of area A_M of the metal under investigation with $Q_M=6\pi^2 V/\lambda A_M c R$. Here V is the volume of the cavity, λ is the wavelength of the radiation, c is the velocity of light, and R is the surface resistance of the cavity walls. Since the $1/Q$'s are power losses, which are additive, the quality factor Q_T for the whole cavity is given by

$$1/Q_T=1/Q_H+1/Q_B+1/Q_M.$$

The fraction P/P_0 of the incident power P_0 which is absorbed in the bolometer is given by

$$P/P_0=Q_T/Q_B=1/(1+\zeta+\eta), \qquad (1)$$

where $\zeta=Q_B/Q_M$ represents the losses in the cavity walls, and $\eta=Q_B/Q_H$ the losses out the coupling hole, both normalized to the losses in the bolometer.

In this experiment we wish to measure the change in the surface resistance R which occurs when the superconductivity is destroyed by a magnetic field. Since our sensitivity is limited by detector noise, we wish to maximize dP/dR. Assuming that the bolometer and the coupling hole look like black holes of the same size so that $Q_H=Q_B$, the optimum cavity is that for which $Q_H=2Q_M$. That is, half the absorption should be in the cavity walls. In terms of the areas of the coupling hole and the cavity walls, the condition is

$$A_H/A_M=\tfrac{2}{3}\mathcal{A},$$

where $\mathcal{A}=cR/\pi$ is the absorptivity of the cavity walls at normal incidence. Estimating the absorptivity of lead under the conditions of the measurement to be about 0.0025, we see that for optimum performance A_M

[12] P. L. Richards, Ph.D. thesis, University of California (unpublished); D. M. Ginsberg, Ph.D. thesis, University of California (unpublished).

[13] R. C. Ohlmann, P. L. Richards, and M. Tinkham, J. Opt. Soc. Am. 48, 531 (1958).

[14] W. E. Lamb, Jr., Phys. Rev. 70, 308 (1946).

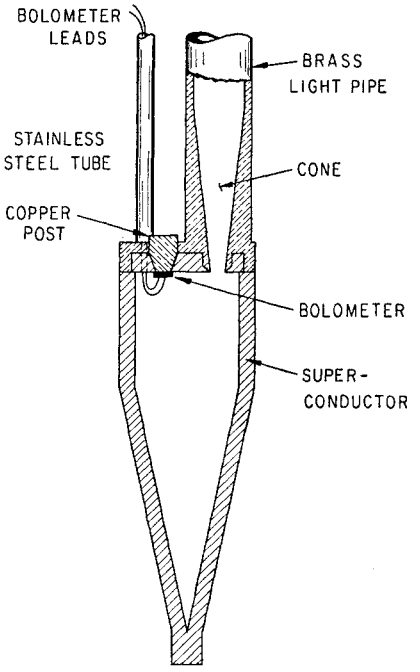

FIG. 2. Plan of nonresonant cavity made from superconductor being studied. The conical cavity shape maximized the absorption in the cavity; the cone in the light pipe decreased the size of the coupling hole.

$=600A_H$. If the light pipe were to terminate directly at the cavity, the required cavity area would be 100 square inches. As Fig. 2 shows, we used a condenser cone similar to the one described by Williamson[15] in order to reduce the diameter of the coupling hole to $\frac{1}{8}$ inch without losing any substantial fraction of the radiation coming down the light pipe. The required cavity area was thus reduced to ~ 7 square inches, an easily obtainable value.

The analysis given above assumes that the photons are randomly distributed in the cavity. Actually, though the cone increases the solid angle of the incoming radiation to 2π, a cavity with a flat bottom would lose many photons to the bolometer or coupling hole after only one or two reflections. To avoid this, the conical cavity design shown in Fig. 2 was used. The cavity shape was adjusted so that photons entering at any angle made between 10 and 14 reflections before returning to the top of the cavity where the coupling hole and bolometer were located. This maximized the average probability of absorption of a photon by the metal for a given cavity size. The cavity dimensions chosen were a length of 4 inches, an inside diameter of 13/16 inch at the large end, and a subtended angle of the cone of 15 degrees, giving a surface area of ~ 7 square inches.

The actual cavity response achieved was limited by persistent current loops enclosing magnetic flux in the cavity walls. This trapped flux kept 5 to 50% of the walls in the normal state at all times after the magnet was first turned on. The evidence for this was that P_S never returned to its full value after the magnet had been turned on, unless the cavity was first warmed up above T_c. Flux trapping was the worst for strained or impure cavities, and appeared to remain constant throughout any one run.

The cavity analysis given above predicts a 100% change in bolometer signal at low frequencies when the cavity walls enter the lossless superconducting state. Experimentally we measure changes of the order of 25% for lead, indicating that much less than half of the radiation was being absorbed in effective regions of the cavity walls. The discrepancy can be attributed to additional absorption by imperfections in the walls which did not change as the cavity entered the superconducting state, to trapped flux which rendered 20% of the cavity area ineffective, and, possibly, to an overestimate of the low-temperature absorptivity of lead. Metals such as tin with smaller absorptivities gave changes in bolometer signal as small as 5%. This range of signals provided one simplification, since with such small changes, as will be shown below, we can use a linear interpretation of the cavity response in terms of the surface resistances of the superconducting and normal states.

The fractional change in the bolometer signal as the cavity goes from the superconducting to the normal state is, from Eq. (1),

$$(P_S-P_N)/P_N=(\zeta_N-\zeta_S)/(1+\zeta_S+\eta). \qquad (2)$$

If we assume a random distribution of photons, Lamb's results give us

$$\zeta=\frac{Q_B}{Q_M}=\frac{4cR}{3\pi}\frac{A_M}{A_B},$$

which is proportional to the surface resistance. In our cavity the photons are not distributed completely at random, but since the power absorbed in the cavity walls is a small fraction of P_0, we may assume that the photon distribution is roughly the same in the superconducting and normal states. In this case ζ will be proportional to R with some constant of proportionality γ. We have from Eq. (2)

$$\frac{P_S-P_N}{P_N}=\frac{R_N(\omega)-R_S(\omega)}{[(1+\eta)/\gamma]+R_S(\omega)}. \qquad (3)$$

For temperatures $T\ll T_c$ and some frequency $\omega_0<\omega_g$, $R_S=0$, so that we can evaluate the constant $(1+\eta)/\gamma$ experimentally from the relation

$$\left.\frac{P_S-P_N}{P_N}\right|_{\omega=\omega_0}=\frac{\gamma R_N(\omega_0)}{1+\eta}. \qquad (4)$$

Thus Eq. (3) gives the response of the cavity in terms of the surface resistances of the cavity walls in the

[15] D. E. Williamson, J. Opt. Soc. Am. 42, 712 (1952).

superconducting and normal states and an experimentally determined constant. We can make one further approximation which is valid for small signals. When $[(P_S-P_N)/P_N]_{\omega_0}$ is small, Eq. (4) shows us that $R_N(\omega_0)\ll(1+\eta)/\gamma$. Thus, since $R_S(\omega)\lesssim R_N(\omega_0)$ over the region of interest, we may neglect $R_S(\omega)$ in the denominator of Eq. (3). It follows that $(P_S-P_N)/P_N$ is nearly proportional to the difference between the surface resistances of the normal and superconducting states.

C. Detection System

A carbon resistance bolometer similar to the one described by Boyle and Rodgers[16] was used as a detector of the far-infrared radiation. The bolometer consisted of a 0.020×0.08×0.2-inch block cut from a 150-ohm, $\frac{1}{2}$-watt Gerard-Hopkins carbon resistor. The carbon was cemented to a 0.008×0.08×0.2-inch sheet of Mylar with General Electric 7031 cement, and the Mylar was in turn cemented to a copper post that came in contact with the liquid helium. The thickness of the Mylar was chosen in order to make the thermal time constant of the bolometer approximately equal to the reciprocal of the angular frequency at which the light was chopped. (The copper post was used because it was found that when the bolometer was mounted on the cavity wall, the difference between the thermal conductivities of the superconducting and normal states was sufficient to change the operating point of the bolometer, and give a spurious signal.) The cavity and light pipe were evacuated to a pressure of less than 10^{-5} mm of mercury so that the thermal contact between the bolometer and the helium bath through the gas was negligible. Electrical contact was made by evaporating indium electrodes onto the ends of the bolometer, and soldering No. 40 manganin wire leads to the indium. Manganin was used so that the thermal conductance of the electrical leads would be negligible compared to that of the Mylar. The arrangement of the bolometer in the cavity is shown in Fig. 2. The bolometer leads were brought to the top of the Dewar in a $\frac{1}{8}$-inch diameter stainless steel tube so that the vacuum seal could be made at room temperature.

A bias current of a few microamperes was supplied to the bolometer by a 22$\frac{1}{2}$-volt battery and an adjustable series resistor. The alternating voltage developed across the bolometer was fed through a blocking capacitor and resonated transformer into a conventional 9 cps lock-in amplifier and chart recorder. The lock-in was driven by a switch attached to the chopper wheel shaft to provide synchronous rectification.

A typical bolometer had a resistance of 600 ohms at room temperature, and 0.1 megohm at 1.4°K. The best signal-to-noise ratio was obtained with a series resistor of 2 to 3 megohms. With the electrical system described above, the bolometer noise was comparable to the amplifier noise for all but a few exceptionally quiet bolometers. The bolometers were not affected by cycling between room temperature and helium temperature, but tended to become very noisy when heated to the melting point of the indium, as occasionally happened while sealing the cavity with Wood's metal. Also, it proved necessary to put a ballast tank in the He pumping line to eliminate noise from temperature fluctuations at the pump frequency.

This experiment would have been extremely difficult without carbon resistance bolometers. Before the bolometers came to the authors' attention, the experiment was attempted using a transmission cavity with a second light pipe to bring the radiation up to a Golay pneumatic detector at the top of the Dewar. The signal-to-noise ratio was so poor that it took several hours to detect any difference between the superconducting and normal states. The bolometers improved the signal-to-noise ratio by more than a factor of 50. The improved geometry possible with the bolometer may have accounted for a factor of 5, but it is clear that the bolometers used were at least an order of magnitude more sensitive than the Golay cell.

In order to measure the temperature dependence of the superconducting energy gap, it was desirable to measure the frequency dependence of $(P_S-P_N)/P_N$ at a variety of temperatures below the critical temperature. We could not use the apparatus described above at temperatures much above 1.5°K, since the bolometer lost its sensitivity rapidly as the temperature was raised. This was due to both a rise in the bolometer's specific heat, and to a fall in its temperature coefficient of resistance. The apparatus shown in Fig. 3 was therefore designed to keep the bolometer temperature low while measurements were made with the cavity at temperatures up to 5°K. A copper cold finger attached to a small helium tank determined the bolometer's temperature. Thermal isolation of the bolometer and helium tank from the rest of the system was achieved by evaluating the cavity. The helium tank was supported, filled, and pumped through a single $\frac{1}{8}$-inch diameter thin-walled stainless-steel tube. The heat leak into the helium tank was small enough that temperatures of the order of 1°K could be reached. This resulted in an increase in bolometer sensitivity compared to that obtainable with the apparatus shown in Fig. 2. The increased sensitivity roughly compensated for the lower cavity Q due to the loss of photons out the annular space around the cold finger.

III. SAMPLE PREPARATION

Cavities of the soft superconductors, lead, tin, and indium, were cast in a stainless-steel mold, and vacuum annealed. The cavity lid was, in most cases, an inset of the same superconductor in the brass cavity top, as is shown in Fig. 2. After annealing, the cavities were acid etched very lightly and soldered to the cavity top

[16] W. S. Boyle and K. F. Rodgers, Jr., J. Opt. Soc. Am. 49, 66 (1959).

TABLE I. Details of sample preparation.

Sample	Source	Fabrication method	Stated purity (%)	r before annealing[a]	Annealing time (hours)	Annealing temp. (°C)	r after annealing[a]
Tantalum I	Fansteel Metallurgical Corp.	machined	99.9	24	8 +8	1600 2000	22.4
Tantalum II	Fansteel	rolled from sheet	99.9	···	8 +8	1600 2000	17.3
Niobium	Fansteel	machined	99.7	9.5	15	1800	12
Vanadium	Electro-Metallurgical Corp.	machined	99.7	8.6	19	1400	9
Lead I	Morris P. Kirk	cast	99.95	···	10^3	30	50
Lead II	A. D. Mackay	cast	99.999	···	40	300	5700
Tin I	Morris P. Kirk	cast	99.9	···	18	195	140
Tin II	Vulcan Detinning Corp.	cast	99.9996	···	35	195	6600
Mercury	Ballard Quicksilver Products Inc.	cast	triple distilled	···	60	−56	610
Indium	Indium Corp. of America	cast	99.999	···	20	100	16 500
99% lead 1% bismuth	···	cast	···	···	30	300	25
50% lead 50% tin	···	cast	···	···	86	175	24

[a] See reference 17.

with Wood's metal. No further polishing was done. Attempts were made to electro-polish a tin cavity, but they were not successful because of its awkward shape and large size. Absorption edges were measured for vanadium, lead, and indium cavities with varying degrees of etching, and for two different mercury cavities. The results were the same to within the experimental error, so that for these superconductors at least, the energy gaps measured did not seem to be a function of the sample preparation. Details of sample purity and preparation are given in Table I.

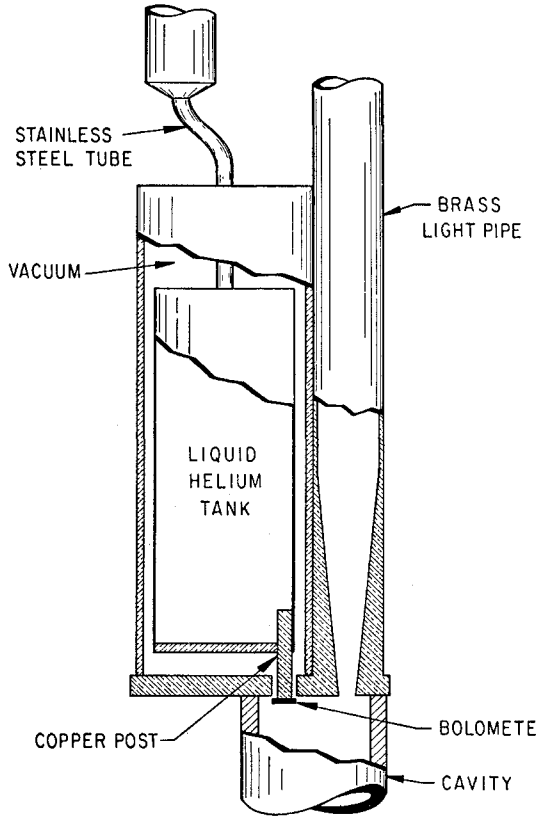

FIG. 3. Apparatus used to measure the temperature dependence of the energy gap. The bolometer's temperature was controlled by the liquid helium in the tank, and its leads passed through a $\frac{1}{8}$-inch diameter stainless-steel tube to the top of the dewar. The tube is behind the plane of the diagram and is not shown.

The mercury cavity required special handling. The cavity was made by filling the stainless-steel mold and immersing it in liquid nitrogen. The cavity lid was frozen in a similar way. Of course, the mercury surface could not be etched. It was cooled slowly over the period of an hour and annealed at dry-ice temperature to minimize strains. After annealing, the cavity was put into a thin-walled brass can which was then soldered to the brass cavity top with Wood's metal in order to complete the vacuum seal. A coil spring in the bottom of the brass can forced the cavity up against the lid to give it good thermal contact with the helium bath. The whole assembly had to be done rapidly to prevent the cavity from melting, and to prevent too much ice from condensing on the cavity walls.

Cavities of the hard superconductors, tantalum, niobium, and vanadium, were machined from one-inch-diameter rods, and annealed at 10^{-5} to 10^{-6} mm pressure in a vacuum induction furnace. Ideally these samples should have been annealed in much higher vacua because there was a marked gettering action as they cooled off in the furnace. In spite of this, the resistance ratios[17] for these metals were generally

[17] The ratio r of the resistance of a sample at room temperature to that at 4.2°K is a measure of the effect of impurities and defects in the metal lattice on the conduction electrons. When we measured resistance ratios for metals that were superconducting at 4.2°K, we destroyed the superconductivity by applying a magnetic field. A plausible extrapolation was made to correct for the magnetoresistance which was quite large in the pure

TABLE II. Values of the energy gap.[a]

Superconductor	T_c (°K)	$10^3 T_c/\Theta_D$	$E_g(0)/kT_c$ present measurements	$E_g(0)/kT_c$ Ginsberg and Tinkham	$E_g(0)/kT_c$ Goodman I	$E_g(0)/kT_c$ Goodman II	$E_g(0)/kT_c$ Goodman III
Indium	3.39	31	4.1±0.2	3.9±0.3	3.5	3.9	
Tin	3.73	19	3.6±0.2	3.3±0.2	3.6	3.6	3.3
Mercury	4.15	52	4.6±0.2		3.7		
Tantalum	4.39	18	≦3.0		3.6	3.6	
Vanadium	5.1	15	3.4±0.2		3.6	3.6	3.5
Lead	7.15	76	4.1±0.2	4.0±0.5	3.9		
Niobium	9.0	35	2.8±0.3		3.7	4.0	3.9

[a] Measured values of the gap at absolute zero, in units of kT_c, compared to values obtained by Ginsberg and Tinkham from transmission measurements on thin films, and by Goodman: I from Eq. (5) with experimental values of γ, H_0, and T_c; II by fitting an exponential function to the experimenta specific heat data; and III by fitting the BCS theory to the experimental specific heat data.

increased by the annealing process. An accident occurred during the annealing of the tantalum cavity that brought the sample to atmospheric pressure of water vapor when it was at 2000°K. An extremely hard layer was formed on the surface of the tantalum. This layer was machined off and the sample was reannealed and acid etched (as far as possible) in hot hydrofluoric acid. This explains why the resistance ratio for the sample tantalum I is slightly smaller after annealing than before. A second tantalum cavity (tantalum II) was made by wrapping a piece of annealed 0.005-inch thick tantalum sheet into a cone. The sheet was somewhat work hardened during the process of making the cone. The tantalum, niobium, and vanadium cavities were mounted in the brass can used for the mercury cavity to avoid having to solder to these metals. The cavities were supported by a coil spring, and thermal contact was improved by filling the space between the cavity and the can with mercury.

Cavities of lead-tin and lead-bismuth alloys were cast in the stainless-steel mold, quenched, and annealed as shown in Table I.

The critical temperatures of our indium, tin I, mercury, and tantalum I samples that are given in Fig. 4 and in Table II were measured using a simplified version of the apparatus described by Cochran, Mapother, and Mould.[18] The actual measurements were made on long ellipsoidal rods that were fabricated and annealed along with the cavities. The mistreatment of tantalum I was not sufficient to change its critical temperature from the value, 4.39°K, found by White, Chou, and Johnston[19] for annealed Fansteel tantalum. The critical temperatures of vanadium, lead, and niobium were too high to measure with our apparatus. The values listed in Table II are those given in the literature for similarly prepared samples. The estimated limits of error of $E_g(0)/kT_c$ for niobium were increased to include the range of critical temperatures reported.

IV. ENERGY GAPS IN PURE SUPERCONDUCTORS AT ABSOLUTE ZERO

Figure 4 shows the curves of $(P_S-P_N)/P_N$ plotted as a function of frequency in wave numbers for seven

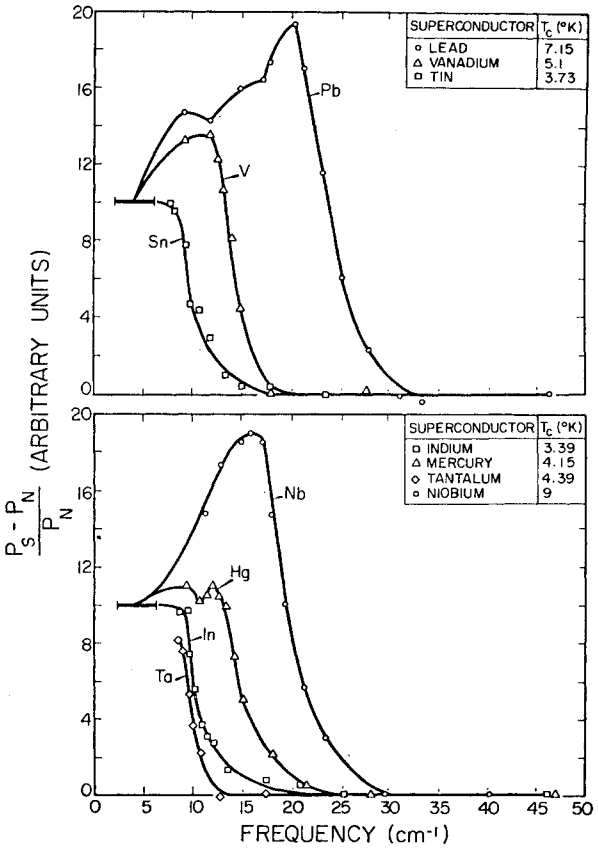

FIG. 4. Low-temperature absorption curves for seven pure superconductors plotted as a function of frequency in wave numbers. These curves have been normalized for display purposes so that the ordinate of the lowest frequency point is the same for each. This point is obtained by using the coarsest dispersion grating in zero order. The estimated spread of frequencies is indicated by the horizontal bar. All other points have band widths of the order of 10%.

samples. The ratio for mercury was measured between just below its melting point and 4.2°K. The resistance ratios r for all of our samples are given in Table I.

[18] J. F. Cochran, D. E. Mapother, and R. E. Mould, Phys. Rev. **103**, 1657 (1956).

[19] D. White, C. Chou, and H. L. Johnston, Phys. Rev. **109**, 797 (1958).

superconductors. The measurements were made at 1.32°K for tantalum, 1.45°K for tin, 1.33°K for indium, 1.28°K for vanadium, 1.32°K for mercury, 1.38°K for niobium, and 1.40°K for lead. The measurements were made by selecting a wavelength using the monochromator and then turning a magnetic field roughly double the critical field on and off every two to five minutes. The frequency of switching depended upon the electronic time constant being used. The values of $(P_S-P_N)/P_N$ obtained by switching the magnet 6 to 20 times, depending upon the noise, were then averaged to obtain a single point.

The preparation of the samples used for these curves is given in Table I. In the cases of tantalum, tin, and lead, where there are two cavities listed, the first one was used. Tantalum II proved to be so strained or impure that it gave a smeared-out absorption edge similar to those of the alloy cavities. The spectroscopically pure cavities tin II and lead II were not used because of what appeared to be an extremely large positive magnetoresistance. P_N, the power that reached the bolometer when the cavity was in a magnetic field greater than H_c, was a very sensitive function of the field. The magnet used could not be controlled well enough to give reproducible measurements of P_N.

We showed in Sec. II that $(P_S-P_N)/P_N$ is roughly proportional to R_N-R_S, the difference between the surface resistances of the superconducting and normal states. Thus, for quantum energies below the energy gap, the curves in Fig. 4 show the difference between the vanishingly small surface resistance of the superconducting state, and the frequency-dependent surface resistance of the normal state. For vanadium, for example, R_s is negligible below ~ 12 cm^{-1}. At quantum energies high enough to excite electrons across the energy gap, there is a sudden onset of absorption in the superconductor, and as the surface resistance approaches that of the normal state, R_N-R_S, and thus $(P_S-P_N)/P_N$, falls rapidly to zero. This rapid approach to the normal-state value of the absorption makes it clear why earlier measurements[7] with room-temperature black-body radiation peaked near 700 cm^{-1} revealed no difference in absorption between the superconducting and normal states. The curves for lead and mercury show structure below the main absorption edge. Several possible interpretations of this structure will be given in the next section. In order to obtain values for the width of the energy gap, we ignore the structure and use the start of the main absorption edge where the curves of Fig. 4 drop steeply and monotonically to zero. In the case of mercury where the main absorption edge is somewhat rounded, we have extrapolated the curve to a sharp corner to obtain the value of the energy gap.

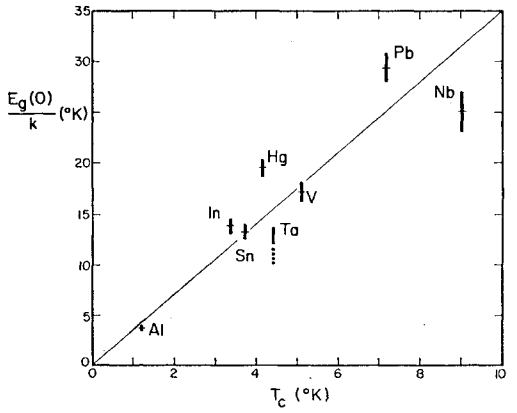

FIG. 5. Measured values of the width of the energy gap at absolute zero in temperature units plotted as a function of the critical temperature. The straight line is the prediction, $E_g(0)=3.5\ kT_c$, of the Bardeen-Cooper-Schrieffer theory. The width of the energy gap of aluminum measured by Biondi and Garfunkel using the microwave surface resistance method is given here, and in the following two figures, for comparison with our data.

The onset of the main absorption edges gives us values of $E_g(T)$, the energy gap at the temperature T at which the data were taken. From these values of $E_g(T)$ we have found the values of $E_g(0)$, the energy gap at absolute zero in units of kT_c listed in Table II, by using the temperature dependence of the energy gap shown in Fig. 10, which comes from the BCS theory. The extrapolation to absolute zero adds only $\sim 0.1\ kT_c$ to $E_g(0)$ for tin and indium, and is negligible for the other superconductors. This list of energy gap values is probably the most important result of these measurements. The errors given are estimated limits of experimental error.

The BCS theory predicts an energy gap at absolute zero of width $3.5\ kT_c$ for all superconductors. Our results show rather large deviations from this law of corresponding states which are well outside our estimated limits of experimental error. In fact, the absorption edges shown in Fig. 4 do not even come in order of critical temperature. In Fig. 5 we have plotted the measured values of the width of the energy gap as a function of the critical temperature. The gap width in aluminum found by Biondi and Garfunkel[6] from microwave surface resistance measurements is also plotted for comparison. The straight line has a slope of 3.5 and so is the prediction of the BCS theory. Certainly $3.5\ kT_c$ is a good average value of the energy gap and there is no systematic deviation as a function of T_c.

Goodman[20] has suggested that since the simple BCS theory is valid only in the weak coupling limit where the critical temperature is assumed to be much smaller than the Debye temperature, deviations from the BCS law of corresponding states might be a smooth function of T_c/Θ_D. He has supported this idea by deducing values of the energy gap from the critical field H_0, the critical temperature T_c, and the normal state electronic specific heat constant γ, using a relation obtained from the

[20] B. B. Goodman, Compt. rend. **246**, 3031 (1958).

BCS theory which he assumes to be independent of the weak coupling limit. This relation is

$$\frac{E_g(0)}{kT_c}=\frac{2H_0}{T_c}\left(\frac{\pi}{6\gamma}\right)^{\frac{1}{2}}. \tag{5}$$

Goodman's values of $E_g(0)/kT_c$ do indeed show a roughly monotonic variation with T_c/Θ_D. We have plotted our measured values of $E_g(0)/kT_c$ as a function of T_c/Θ_D in Fig. 6. We do not find the expected monotonic variation.

One might expect that Eq. (5) would be more reliable than the BCS relation $E_g(0)=3.5\ kT_c$ because it contains only quantities defined at absolute zero, and so does not depend upon the thermodynamics of the BCS model. The agreement between theory and experiment is not, however, significantly improved when one plots our values of $E_g(0)$ as a function of $H_0/\sqrt{\gamma}$.

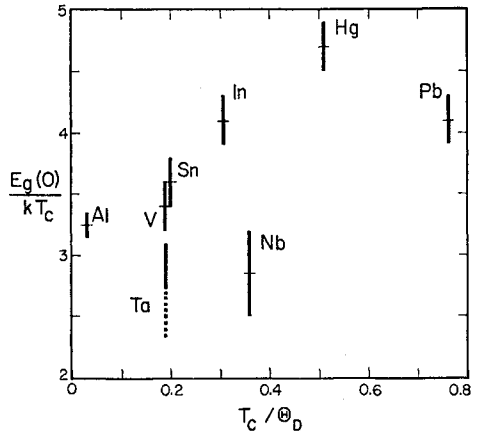

FIG. 6. Measured values of the width of the energy gap at absolute zero divided by kT_c plotted as a function of the ratio of the critical temperature to the Debye temperature.

In Fig. 7 we have plotted $E_g(0)/kT_c$ as a function of the Debye temperature alone. Here we appear to have a somewhat better fit to a monotonic function. This is, however, a strictly empirical observation, and it is difficult to see how such a functional relationship would arise in a theory of the BCS type.

The electronic specific heats of a number of superconductors have been measured as a function of temperature. Over the range $2.5<T_c/T<6$, the BCS theory predicts an exponential specific heat of the type expected from a simple energy gap model. The slope $-b$ of $\log C_{es}/\gamma T_c$, when plotted as a function of T_c/T, is predicted to have the value -1.44. The experimental data are only roughly exponential over this temperature range.[2,21] The specific heat at temperatures much lower than T_c is generally larger than is expected from a simple energy gap. This effect may be

[21] H. A. Boorse, Phys. Rev. Letters **2**, 391 (1959).

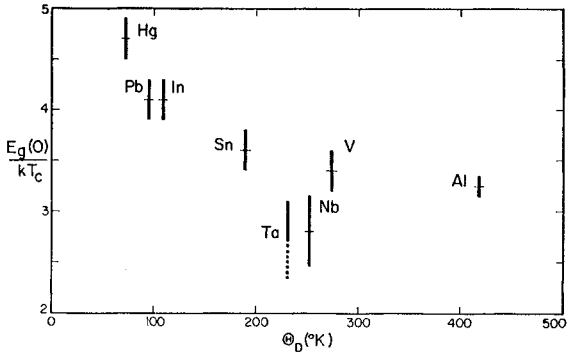

FIG. 7. Measured values of the width of the energy gap at absolute zero divided by kT_c plotted as a function of the Debye temperature.

explained by an anisotropic gap of the type deduced by Morse, Olsen, and Gavenda[22] from ultrasonic attenuation data. Because of this complication, it is difficult to obtain an unambiguous value of the energy gap from the experimental data. Goodman[23] has surveyed the most recent specific heat work and has obtained values of the energy gap by two methods. One was to fit an exponential to the data and to obtain the gap from the formula $E_g(0)/kT_c=3.5b/1.44$, which comes from the BCS theory. The other was to fit the whole BCS specific heat curve to the data using $E_g(0)$ as an adjustable parameter. His results for the superconductors that we have measured are given in the last columns of Table II. The agreement with our measurements is reasonably good except for tantalum, niobium, and mercury.

Our measured values of the energy gaps of tantalum and niobium could be in error because of the poor quality of the surfaces used. The absorption edges for these metals are sharp, indicating that the energy gap has the same value over the whole cavity surface. Ittner and Marchand[24] have shown that dissolved gas has a pronounced effect on T_c for tantalum. Thus, gas dissolved in the surface layer as the tantalum and niobium cavities cooled after annealing, which would not affect the measured T_c of the bulk sample, could uniformly change the measured gap.

Our value for the mercury gap is more reliable, since two different cavities were measured with the same results. The disagreement between our mercury gap and the one obtained by Goodman[20] from Eq. (5) or from a monotonic variation of the gap as a function of T_c/Θ_D may be related to the fact that mercury does not follow the Debye specific heat law at all well at low temperatures. Its Debye temperature drops from 80°K to 50°K as the temperature is raised from zero to T_c.

[22] R. W. Morse, T. Olsen, and J. D. Gavenda, Phys. Rev. Letters **3**, 15 (1959).

[23] B. B. Goodman, paper presented at Superconductivity Conference, Cambridge, June, 1959 (unpublished).

[24] W. B. Ittner and J. F. Marchand, Phys. Rev. **114**, 1268 (1959).

Ginsberg and Tinkham[10] have deduced values of $E_g(0)/kT_c$ from their measurements of the transmission of thin superconducting films. Their values are also given in Table II, and they are in quite good agreement with our values. It is perhaps remarkable that the energy gap width in a film of the order of 10–20 angstroms in thickness is the same as in the bulk metal.

V. STRUCTURE ON THE ABSORPTION EDGES OF MERCURY AND LEAD

As we were measuring the absorption curves for mercury and lead, we noticed structure at frequencies below the main absorption edge. This structure was only slightly larger than the random scatter of the data and so was not fully believed to be real until evidence for a similar effect in lead films was found by Ginsberg and Tinkham.[25] The mercury and lead curves of Fig. 4, which show the structure, are the results of averaging a number of runs, each of which showed the dip below the main absorption edge.

Since $(P_S-P_N)/P_N$ is roughly proportional to the difference between the surface resistances of the normal and the superconducting states, the dips could be caused by an absorption in the superconducting state at frequencies below the main gap edge, or by dips of the surface resistance in the normal state. The structure was independent of the magnetic field used to destroy the superconductivity. This fact, along with the modest quality of the samples, rules out the possibility that we observed a magnetic resonance type of effect in the normal state. We interpret the structure as absorption in the superconducting state caused either by isolated states in the superconducting energy gap, by an extremely anisotropic gap (such as two separate gaps for different pieces of Fermi surface), or just possibly by a dielectric anomaly.

The sharpness of the observed dip, especially in the case of mercury, would seem to indicate a discrete absorption line separated from the main absorption edge. Such a discrete absorption could obviously arise from a discrete set of states in the energy gap. However, because the absorption comes superimposed on the rising curve of the normal state surface resistance whose exact shape is not known, we really cannot rule out the possibility that the structure is due simply to a smaller gap for creation of excitations on certain parts of the Fermi surface.

We find evidence for absorption below the main gap edge only for mercury and lead, which have the largest values of T_c/Θ_D, and thus the strongest electron-phonon interactions of any superconductors. Our frequency range is restricted enough that we would not notice such an effect if it occurred in indium, tin, or tantalum, but we probably would have observed it in niobium or vanadium. The correspondence between our measured structure and that deduced from the film transmission data is very close. The structure has been observed in both lead and mercury films, and its position relative to the main gap edge is the same as in the bulk experiments.[25]

Other relevant experimental information comes from specific heat data. The electronic specific heats of superconducting mercury and lead, as derived from critical field measurements,[26] differ markedly from those of other superconductors. Their specific heat is much larger at low temperatures than is predicted by the BCS theory. This is exactly the effect that would be expected from a significant group of states with a smaller energy gap that would accordingly play an important part in the thermal excitations at low temperatures.

Next, let us consider the theoretical situation. In the simple BCS theory, the quantity $V_{\mathbf{k}\mathbf{k}'}$ which gives the interaction between pairs with momenta $\mathbf{k}$ and $\mathbf{k}'$, is arbitrarily set equal to a constant V. This leads to a single unique gap value. Anderson[27] has shown that if this assumption is relaxed, and $V_{\mathbf{k}\mathbf{k}'}$ is assumed to depend upon $\mathbf{k}$ and $\mathbf{k}'$, there may be collective excitations from the superconducting ground state with excitation energies less than the BCS gap. It is possible that our observed structure is due to collective excitations of the type discussed by Anderson. It remains to be seen, however, whether the transition probabilities are such that these excitations can account for the observed optical effects. It also seems highly unlikely that the density of states in the gap due to the collective excitations could be large enough to account for the observed specific heats of lead and mercury.

Another result of assuming $V_{\mathbf{k}\mathbf{k}'}$ to vary with $\mathbf{k}$ and $\mathbf{k}'$ in the BCS theory is, as has been pointed out by Cooper[28] and by Anderson,[29] that the predicted energy gap is anisotropic. Suhl and co-workers[30] have worked out a detailed example of this sort, in which they consider two separate pieces of Fermi surface with the distinct gaps. This treatment shows that the widths of the two gaps would be expected to go to zero at a common transition temperature. Cooper has suggested that this gap anisotropy explains both the nonexponential specific heats and the anisotropic energy gap deduced from ultrasonic attenuation measurements in tin by Morse, Olsen, and Gavenda.[32] It is also possible that the structure that we observe on the absorption curves of mercury and lead is due to this anisotropy, since two distinct gaps could even cause structure as sharp as that on our mercury curve. The anisotropy in lead and mercury would have to be more pronounced than that of the other superconductors in order to account for their anomalous specific heats. Anisotropy of the gap

[25] D. M. Ginsberg, P. L. Richards, and M. Tinkham, Phys. Rev. Letters, **3**, 337 (1959).

[26] D. L. Decker, D. E. Mapother, and R. W. Shaw, Phys. Rev. **112**, 1888 (1958); D. K. Finnemore, D. E. Mapother, and R. W. Shaw, Phys. Rev. **118**, 127 (1960).

[27] P. W. Anderson, Phys. Rev. **112**, 1900 (1958).

[28] L. N. Cooper, Phys. Rev. Letters **3**, 17 (1959).

[29] P. W. Anderson, Bull. Am. Phys. Soc. **4**, 148 (1959).

[30] H. Suhl, B. T. Matthias, and L. R. Walker, Phys. Rev. Letters **3**, 552 (1959).

would affect the exponential nature of the specific heat strongly only if the smaller gap applied to a relatively small part of the Fermi surface. The small gap would then dominate at low temperatures, but at higher temperatures the gap with the larger statistical weight would dominate. If, on the other hand, the smaller gap applied to the majority of the Fermi surface, very little effect of the small bit of surface with a larger gap would appear either thermally or in electromagnetic absorption.

Anderson[29] has proposed a reason why the anisotropy of the energy gap should not be observable in our measurements. He has considered the effects of impurity scattering on theories of the BCS type. Rather than diagonalizing the BCS Hamiltonian with the plane waves that describe electrons in a pure superconductor, he attacked the problem starting with the linear combinations of plane waves that describe the electrons in the presence of many elastic scattering centers. One result is that the interaction $V_{\mathbf{k}\mathbf{k}'}$ is averaged over the whole Fermi surface so that no anisotropy is expected. Anderson estimates that the scattering will be strong enough to make his approach valid if $\omega_0\tau<1$. In the next section we estimate values of $\omega_0\tau$ for our samples (see Table III). The mercury and the indium cavities are too pure for this "dirty superconductor" theory to be valid in the interior, but surface scattering may reduce $\omega_0\tau$ to less than unity within the skin depth. The other cavities all have $\omega_0\tau\lesssim 1$, so that Anderson's theory seems to offer an adequate explanation of why we would not observe the anisotropy of the gap that has been seen by Morse, Olsen, and Gavenda in tin.

A possible reconciliation of these various arguments would be obtained by assuming Anderson's averaging to occur only within the two separate pieces of Fermi surface imagined by Suhl. This would lead to two sharp gaps which could explain our data on lead and mercury, and also explain the nonexponential specific heats for the same metals. Further, in the interior of the very pure samples used by Morse, Olsen, and Gavenda, presumably no averaging at all occurs, and the full anisotropy of the gap is manifest. If, on the other hand, one attributes the structure to exciton-like discrete states in an averaged gap, then the correlation with the nonexponential specific heats is left unresolved, except insofar as Hg and Pb share the distinction of having a very strong electron-phonon interaction, which makes T_c/Θ unusually large.

VI. DEPENDENCE OF THE ENERGY GAP UPON TEMPERATURE AND MAGNETIC FIELD

In order to obtain an experimental check of the temperature dependence of the energy gap predicted by the BCS theory, we measured the absorption edges of lead and vanadium at a variety of temperatures below T_c using the apparatus shown in Fig. 3. The resulting curves of $(P_S-P_N)/P_N$ as a function of reduced

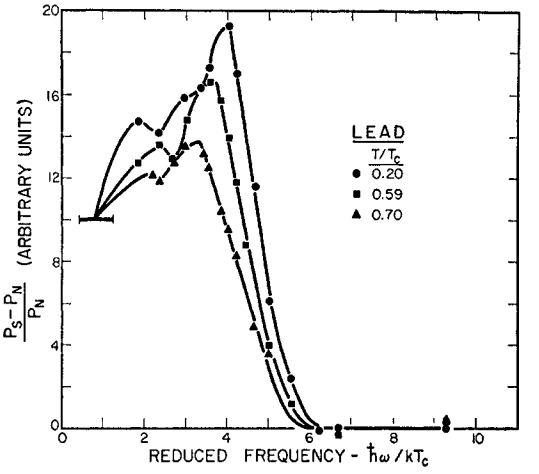

FIG. 8. Absorption curves for lead as a function of temperature. These data, and those in Fig. 9, have been normalized as was done in Fig. 4.

frequency $\hbar\omega/kT_c$ are given in Figs. 8 and 9. The $T/T_c=0.70$ curve for lead corresponds to 5.0°K, which was the highest temperature that we could reach by applying an overpressure to the liquid helium surrounding the cavity. The highest temperature curve for vanadium was measured at 4.2°K. Higher temperatures could have been reached, but the absorption edge would have come at too low a frequency for us to measure. Even for the 4.2°K curve it was necessary to interpolate, using the shapes of the lower temperature curves, to find the width of the energy gap.

The temperature dependence of the energy gaps of lead and vanadium are compared to the prediction of the BCS theory in Fig. 10. It can be seen that our data agree with the BCS temperature dependence to well within the experimental error.

One expects from the Kramers-Kronig[31] relations

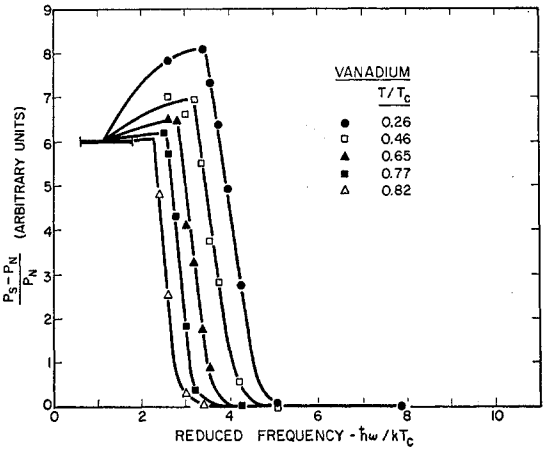

FIG. 9. Absorption curves for vanadium as a function of temperature.

[31] R. de L. Kronig, J. Opt. Soc. Am. 12, 547 (1926); H. A. Kramers, Atti. congr. intern. fis. Como 2, 545 (1927).

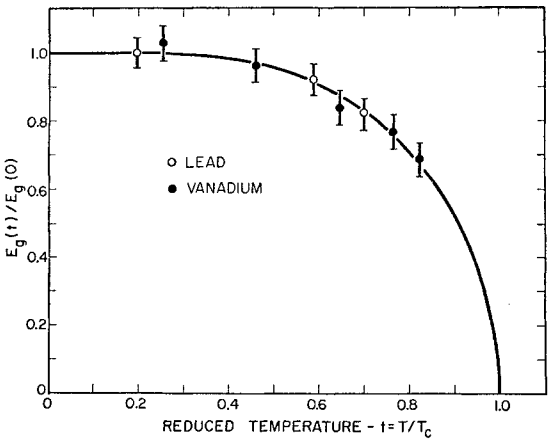

FIG. 10. The temperature dependence of the energy gaps of lead and vanadium. The solid curve is the prediction of the Bardeen-Cooper-Schrieffer theory. In both cases, $E_g(0)$ was chosen for a best fit to the theoretical curve.

that the sudden rise of the surface resistance at the gap frequency should be anticipated by a rise in the imaginary part of the surface impedance, the surface reactance. The surface reactance determines the penetration of fields into the superconductor. Hence, at high temperatures where normal electrons are present one might expect an increased absorption due to an increase in penetration depth at frequencies just below the gap frequency. This effect has been examined in detail by Biondi and Garfunkel[32] who find that it is negligible in aluminum below 0.7 T_c, and is small for higher temperatures. Assuming that the effect is roughly the same in all superconductors because of the similarity of the absorption edges, we expect that there might be an error in our highest temperature vanadium point due to this cause. It should, however, be small compared to the other experimental errors.

The temperature dependence of the energy gap has been deduced by Morse and Bohm[33] from their measurements of ultrasonic attenuation in tin, and by Biondi and Garfunkel[6,32] from their measurements of the surface resistance of aluminum at microwave frequencies. Both experiments agree with the BCS prediction about as well as our data do. Thus it appears that the BCS theory gives the correct temperature dependence of the energy gap for a variety of superconductors. This conclusion justifies our use of the BCS temperature dependence to make the small extrapolation to absolute zero of the values of E_g/kT_c measured at $T \ll T_c$, as was done to obtain the values of $E_g(0)/kT_c$ listed in Table II.

Figure 8 shows the structure on the lead absorption curve at three temperatures. One possible interpretation of these data is that there are two dips which scale with temperature just as the main absorption edge does. Both dips appear, barely resolved, at $T/T_c=0.20$. At the higher temperatures, the lower frequency dip would then shift to such low frequencies that it would not be seen. Considering the random scatter of the data, and the wide spacing between points, the most that we can say is that the data appear to be consistent with such an interpretation.

It has been assumed in the interpretation of this experiment that the energy gap is independent of a magnetic field less than the critical field. The trapped flux in the cavity walls mentioned in Sec. II subjected large areas of the cavity surface to fields of the order of the critical field when the magnet was turned off. The sharpness of the absorption edges, and the fact that they were the same for different cavities of the same metal which had different amounts of trapped flux, supports our assumption that the energy gap is not a sensitive function of such fields.

VII. COMPARISON OF ABSORPTION CURVE SHAPE WITH THEORY

A. Absorption in the Normal State

In pure metals at high frequencies and low temperatures, the electronic mean free path l may become greater than the skin depth δ so that the fields vary considerably over one mean free path. The current at a point is then no longer given by a local relation such as Ohm's law, but by an integral of the field over a surrounding region. In the normal state, the degree to which nonlocal effects are important is determined by the ratio l/δ.[34]

We may estimate values of the ratio l/δ for each of our samples. Using the room temperature conductivities of the metals given in standard references, and the resistance ratios given in Table I, we may obtain the conductivity σ of our samples at helium temperatures. l can then be found directly for lead and tin by using Chambers'[35] values of σ/l. We have made order-of-magnitude estimates of l for the other samples by using the free electron expression for the conductivity $\sigma=ne^2l/mv_0$, and assuming Fermi velocities v_0 of 10^8 cm/sec, and one conduction electron per atom. The ratio of the mean free path to the classical skin depth evaluated at the gap frequency, $\delta_{Cl}=c/(2\pi\omega_g\sigma)^{\frac{1}{2}}$, is given in Table III for each of our cavities. At far-infrared frequencies, the inertia of the electrons may prevent them from following the fields. The importance of inertial effects in our experiment can be estimated by calculating $\omega_g\tau=\omega_g l/v_0$. Order-of-magnitude estimates of this parameter are also given in Table III.

We may determine the valid limit of the skin effect theory from these estimates of l/δ_{Cl} and $\omega_g\tau$ by referring to a chart prepared by Pippard[34] from the calculation

[32] M. A. Biondi and M. P. Garfunkel, Phys. Rev. **116**, 853 (1959).

[33] R. W. Morse and H. V. Bohm, Phys. Rev. **108**, 1094 (1957).

[34] For a review of this subject see A. B. Pippard, *Advances in Electronics and Electron Physics*, edited by L. Marton (Academic Press, Inc., New York, 1954), Vol. 6, p. 1.

[35] R. G. Chambers, Proc. Roy. Soc. (London) **A215**, 481 (1952).

TABLE III. Values of parameters used to determine the valid limit of the skin effect theory.[a]

Superconductor	$\omega_q\tau$	l/δ_{Cl}	ξ_0/λ
Indium	~300	~80 000	~5
Tin I	~2	48	4.2
Mercury	~7	~3000	~7
Tantalum	~0.2	~2	
Vanadium	~0.05	~0.2	
Lead I	~1	5.7	~3
Niobium	~0.2	~1	

[a] In the normal state, the classical theory is valid if $\omega\tau<1$ and $l/\delta_{Cl}<1$. Inertial effects must be considered if $\omega\tau\gtrsim 1$, and nonlocal effects are important if $l/\delta_{Cl}\gtrsim 1$. In the superconducting state, ξ_0/λ determines the importance of nonlocal effects. Our estimates of these parameters were made from the bulk properties of our samples. Surface defects, if large compared to the penetration depth for our acid-etched surfaces, would decrease the effective values of $\omega_q\tau$, l/δ_{Cl}, and ξ/λ from the values given here.

of Reuter and Sondheimer[36] and of Dingle.[36] We find that nonlocal effects are negligible for our vanadium, niobium, and tantalum cavities, and that they are just beginning to be important for lead I. Tin I, mercury and indium, however, all have large enough values of l/δ_{Cl} for the extreme anomalous limit to be valid. $\omega_q\tau$ is large enough for all our cavities except vanadium that inertial effects are beginning to become important. This is especially true in the cases of mercury and indium. For large enough $\omega_q\tau$, the theory predicts that the surface resistance becomes independent of frequency no matter what the value of l/δ_{Cl}. Thus at frequencies as high as ω_q inertial effects should cause $R_N(\omega)$ to rise more slowly than the $\omega^{\frac{1}{2}}$ dependence predicted in the classical limit or the $\omega^{\frac{2}{3}}$ dependence predicted in the extreme anomalous limit.

The absorption mechanism in the skin effect theory discussed thus far consists of electrons absorbing photons and colliding with impurities or with the surface of the metal to conserve energy and momentum. Holstein[37] has suggested that at optical frequencies and low temperatures, electrons might also absorb photons and emit phonons to conserve energy and momentum. This absorption mechanism has not been worked out at far-infrared frequencies, but might be important, especially for superconductors which have large electron-phonon interactions.

B. Absorption in the Superconducting State

The experimental low-temperature absorption edge curves shown in Fig. 4 have a variety of shapes below the gap. We have interpreted these curves as the frequency dependence of R_N-R_S, and, apart from the structure discussed earlier, we have assumed that R_S is negligible for $\omega<\omega_q$. The curves for the metals with lower critical temperatures do not rise as steeply with frequency below the gap as the others. One possible reason for this is that the temperatures used (1.28 to 1.4°K) are not negligible compared to the smaller critical temperatures. In these cases it is possible to get appreciable absorption in the superconducting state below ω_q due to electrons thermally excited across the gap, which would depress R_N-R_S in this region. However, on the basis of the lower frequency microwave data, we expect R_S to be only about 3% of R_N for indium, and much less for the superconductors with higher critical temperatures, so that this effect is probably negligible. A more important effect is that the output of our arc lamp falls off rapidly at low frequencies so that adequate filtering of unwanted radiation is difficult below 10 cm^{-1}. Most of the unwanted radiation is at higher frequencies, especially the second harmonic, so that it would tend to depress the lowest frequency narrow bands points. With the limited filtering possible in these reflection experiments, this effect could be as large as 10% for the very lowest frequencies, and it probably contributes to the flat tops on the lower frequency absorption edges. These experimental and theoretical uncertainties prevent us from predicting the exact frequency dependence of $(P_S-P_N)/P_N$ below ω_q. There is, however, qualitative agreement with the theory. In each case, it appears that $R_N(\omega)$ rises rapidly from zero at zero frequency, and then more slowly near the gap.

In the superconducting state, the importance of nonlocal effects is determined by the ratio of the Pippard[38] superconducting coherence length ξ to the penetration depth λ. Estimates of this ratio are given in Table III for several of our samples. We used the value of the coherence length ξ_0 for pure tin measured by Faber and Pippard,[39] and experimental values of λ for pure superconductors.[40] We estimated ξ_0 for indium, mercury, and lead from Pippard's[38] relation $\xi_0=0.15\hbar v_0/kT_c$. The mean free path in these samples is large enough that λ and ξ should have the values characteristic of pure metals. It is clear that the condition for the validity of the extreme anomalous limit in the superconducting state, $\xi/\lambda\gg 1$, is only partially met, even in our best samples. Inertial effects are also important in the superconducting state. Sturge[41] has found evidence that they may become important at even lower frequencies than in the normal state.

The nonlocal response of a metal can be expressed by a conductivity if all space and time dependent quantities are Fourier analyzed. The ratio of the coefficients of the plane wave $\exp[i(\mathbf{k}\cdot\mathbf{x}-\omega t)]$ in the current density and electric field defines a complex conductivity $\sigma(\omega,k)=\sigma_1(\omega,k)+i\sigma_1(\omega,k)$ which is a function of the magnitude of the wave vector $\mathbf{k}$ as well as the angular frequency ω. The surface resistance R is determined by an average conductivity $\sigma(\omega)$ in which the various values of $\mathbf{k}$ are weighted in proportion to $|E(\omega,\mathbf{k})|^2$.

[36] G. E. H. Reuter and E. H. Sondheimer, Proc. Roy. Soc. (London) **A195**, 336 (1948); R. B. Dingle, Physica **19**, 311 (1953).
[37] T. Holstein, Phys. Rev. **96**, 535 (1954).
[38] A. B. Pippard, Proc. Roy. Soc. (London) **A216**, 547 (1953).
[39] T. E. Faber and A. B. Pippard, Proc. Roy. Soc. (London) **A231**, 336 (1955).
[40] D. Shoenberg, *Superconductivity* (Cambridge University Press, New York, 1952), second edition.
[41] M. D. Sturge, Proc. Roy. Soc. (London) **A246**, 570 (1958).

Thus, in the extreme anomalous limit where the penetration of fields is small, large values of k are important. For these large values of k, $\sigma(\omega,k)$ is proportional to $1/k$ in both the superconducting and the normal states so that the ratio $\sigma_S(\omega,k)/\sigma_N(\omega,k)$ is independent of k. If, in addition, $\omega_g\tau\ll 1$, then $\sigma_N(\omega,k)$ is predominantly real, and we may write $\sigma_S(\omega,k)/\sigma_N(\omega,k)=\sigma_1/\sigma_N+i\sigma_2/\sigma_N$. Mattis and Bardeen[42] have calculated the frequency dependence of σ_1/σ_N and σ_2/σ_N from the BCS theory. In the extreme anomalous limit, R_S/R_N may be found from

$$Z_S/Z_N=[\sigma_N/(\sigma_1+i\sigma_2)]^{\frac{1}{2}}, \tag{6}$$

and

$$Z_N=(1+i\sqrt{3})R_N. \tag{7}$$

Using the fact that R_N is proportional to $\omega^{\frac{2}{3}}$ in this limit, we may deduce the frequency dependence of R_N-R_S. The results are compared to typical absorption edges in Fig. 11. The onset of absorption predicted by Mattis and Bardeen is much more gradual than our observed absorption edges. Most of our samples were not in the extreme anomalous limit so that σ_1/σ_N and σ_2/σ_N may really depend upon wave vector. It appears that the curve of $\sigma_1(\omega,k)/\sigma_N(\omega,k)$, averaged over the important values of the wave vector, rises more rapidly above ω_g than the σ_1/σ_N of Mattis and Bardeen. If we plot the curves of Fig. 4 as a function of frequency in units of the energy gap, and normalize them so that they coincide at ω_g, the differences among the slopes of all our absorption edges is small compared to the deviation from the Mattis-Bardeen slope. This means that despite the wide variation of l/δ_{Cl} and ξ/λ, the effective frequency dependent conductivities are probably very nearly the same for all of our samples. Thus it seems somewhat unlikely that the dependence of the conductivities upon wave vector could be large enough to account for the discrepancy between our results and the prediction of Mattis and Bardeen.

We have investigated how rapidly σ_1/σ_N would have to rise from zero above ω_g in order to agree with the steepness of our absorption edges in the extreme anomalous limit. Our empirical curve of σ_1/σ_N shown in Fig. 12 rises as $1-(\omega_g/\omega)^2$ for $\omega_g<\omega<1.3\omega_g$, and coincides with the Mattis-Bardeen curve for $\omega>4\omega_g$. The imaginary part of the conductivity σ_2/σ_N is found by calculating the Kramers-Kronig transform of the full σ_1/σ_N, including the delta function at $\omega=0$ required by the Ferrell-Glover[43] sum rule. The frequency dependent conductivities obtained in this manner, along with Eqs. (6) and (7), predict the frequency dependence of R_N-R_S shown in Fig. 11.

It should be noticed that the measured absorption curves in Fig. 4 do not ever show more absorption in the superconducting state than in the normal state. Well beyond the energy gap, where $\sigma_1/\sigma_N\gg\sigma_2/\sigma_N$, Eqs. (6) and (7) give us

$$\frac{R_S}{R_N}=\left(\frac{\sigma_N}{\sigma_1}\right)^{\frac{1}{2}}\left(1-\frac{1}{\sqrt{3}}\frac{\sigma_2}{\sigma_1}\right).$$

The experimental fact that R_S/R_N approaches unity from below places some limitations on the high-frequency behavior of σ_1/σ_N and σ_2/σ_N, since R_S/R_N is a sensitive function of both quantities for $\omega\gg\omega_g$. Many of the σ_1/σ_N curves derived by Ginsberg and Tinkham[10] from thin film transmission data rise rapidly from zero at the gap roughly as $1-(\omega_g/\omega)^2$ in a way quite similar to Fig. 12, but they generally approach unity so rapidly that, in contrast to the results of these measurements, they would predict $(R_N-R_S)<0$ over a large range of frequencies if they were to be applied to a bulk metal in the extreme anomalous limit.

In the classical region where Ohm's law is valid, σ_1/σ_N and σ_2/σ_N are again independent of wave vector

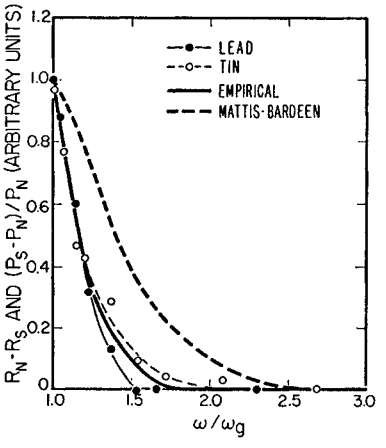

FIG. 11. Experimental absorption edges for lead and tin compared to curves of R_N-R_S calculated in the extreme anomalous limit. The heavy dashed curve is the prediction of the theory of Mattis and Bardeen; the heavy solid curve was derived from the empirical conductivities shown in Fig. 12.

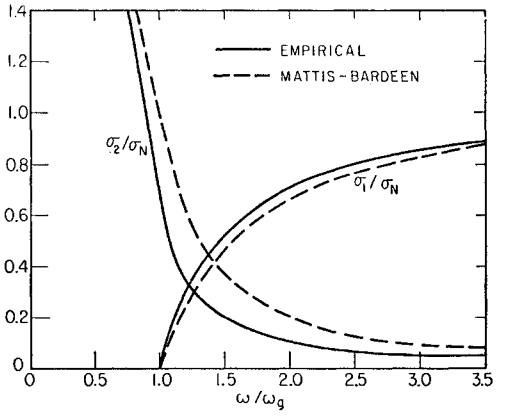

FIG. 12. Empirical frequency-dependent conductivities used to fit the observed absorption edges compared to the Mattis-Bardeen conductivities.

[42] D. C. Mattis and J. Bardeen, Phys. Rev. 111, 412 (1958).

and R_N-R_S may be found from

$$Z_S/Z_N=[\sigma_N/(\sigma_1+i\sigma_2)]^{\frac{1}{2}}, \quad (8)$$

$$Z_N=(1+i)R_N, \quad (9)$$

and the fact that R_N is proportional to $\omega^{\frac{1}{2}}$. In this limit, the conductivities shown in Fig. 12, and those of Mattis and Bardeen (which were derived assuming the extreme anomalous limit), predict that R_N-R_S becomes slightly negative beyond $\omega=1.5\,\omega_g$ and $\omega=2\omega_g$, respectively. The general steepness of the absorption edge is slightly increased by using the classical equations (8) and (9), rather than the extreme anomalous equations (6) and (7). In order to predict absorption edges like those that we measured for vanadium and niobium, σ_1/σ_N would have to rise from zero almost as fast as $1-(\omega_g/\omega)^2$, but then, in order to keep $(R_S-R_N)\leqq 0$, it would have to approach unity slightly more slowly than the Mattis-Bardeen curve. In the classical limit, when $\sigma_1\gg\sigma_2$, it is

$$\frac{R_S}{R_N}=\left[\frac{\sigma_N}{\sigma_1}\left(1-\frac{\sigma_2}{\sigma_1}\right)\right]^{\frac{1}{2}},$$

which we know empirically must approach unity from below for $\omega\gg\omega_g$.

It is conceivable that the structure which we find on the absorption curves of mercury and lead may involve a dielectric anomaly, that is, a peak in the penetration depth due to σ_2 passing through zero. In the presence of a small σ_1 below the gap, an increase in penetration causes an increase in absorption. To investigate this possibility, which was brought to our attention by R. A. Ferrell, we require a general expression for the surface resistance as a function of $\sigma(\omega,k)$. We may transform the expression given by BCS for a penetration depth λ as a function of a k-dependent response function into a surface impedance by using the general relationship $Z=-4\pi i\omega\lambda/c^2$. The result for the surface resistance in the simpler case of specular electron reflection is

$$R=\frac{2}{\pi}\int_0^\infty \frac{\sigma_1(\omega,k)dk}{[(c^2k^2/4\pi\omega)+\sigma_2(\omega,k)]^2+\sigma_1^2(\omega,k)}.$$

Thus we see that if $\sigma_1(\omega,k)$ is small but finite, and $[(c^2k^2/4\pi\omega)+\sigma_2(\omega,k)]$ passes through zero, then there will be a peak in $R(\omega)$. For any given small value of σ_1, the peak is roughly Lorentzian. Its height is $\sim 1/\sigma_1(\omega,k)$ and width $\sim\sigma_1(\omega,k)/a$, where a is the slope of $\sigma_2(\omega,k)$ at the peak frequency, so that the area under the peak is independent of $\sigma_1(\omega,k)$. $\sigma_1(\omega,k)$ is certainly small at $\sim 0.8\omega_g$, where we observe the peak in R_S. In order for this mechanism to explain the observed structure, we would need to have $\sigma_2(\omega,k)\leqq -c^2k^2/4\pi\omega$ at $\sim 0.8\omega_g$ for some value of k. Considering only pure superconductors for which $l\gg\xi_0$ ($\omega_g\tau\gg 1$), such a negative value of $\sigma_2(\omega,k)$ is unlikely for $k\xi_0\ll 1$, where $\sigma_2(\omega,k)$ approaches the value given by the London[44] theory, and for $k\xi_0\gg 1$, where $c^2k^2/4\pi\omega$ becomes prohibitively large. At $k\xi_0\cong 1$, $\sigma_1(\omega,k)$ is nonzero only between ω_g and $\omega=v_0k\cong 2\omega_g$.[3] The cutoff at $\omega=v_0k$ is due to the fact that an electron can absorb energy from a wave only when it remains in phase with it, i.e., only when the phase velocity ω/k is less than v_0. Using the Ferrell-Glover sum rule and the Kramers-Kronig transforms, we can calculate $\sigma_2(\omega,k)$ from $\sigma_1(\omega,k)$. The result is that it is possible, but rather unlikely, that $\sigma_1(\omega,k)$ is peaked high enough to produce a dielectric anomaly for those components of the conductivity for which $k\xi_0\cong 1$.

There is a close correspondence between the dips in our absorption edges and the dips in the film transmission data of Ginsberg and Tinkham.[10] Hence it seems likely that the two effects are due to the same cause. Yet a dielectric anomaly where $\sigma_2=0$ would in fact produce a peak rather than a dip in the transmission. In order for any one mechanism to explain both the film and the bulk results, it must account for a rise in σ_1 rather than a zero of σ_2. Hence, it seems unlikely that a dielectric anomaly is the explanation for the observed structure.

VIII. ALLOY SUPERCONDUCTORS

In order to determine the nature of the energy gap in impure or badly strained superconductors, we made cavities from one-phase and two-phase alloys. The one-phase alloy was 99% lead and 1% bismuth, which has a critical temperature a few tenths of a degree above that of pure lead.[45] The cavity was cast and quenched, and then annealed as shown in Table I. Rapid cooling and then long annealing in the solid state will make this type of alloy homogeneous. Stout and Guttman[46] found that sufficiently annealed one-phase alloys showed superconducting transitions as sharp as those of pure superconductors, rather than the broad transitions characteristic of less well-prepared alloys.

Figure 13 shows the absorption edge for the lead-bismuth cavity plotted against frequency in cm^{-1}. Compared to that of pure lead shown in Fig. 4, where the absorption sets in sharply near 20 cm^{-1}, we see that the onset of absorption is greatly smeared out. This data should not be taken to mean that there is no strict energy gap in a homogeneous superconducting alloy. The thickness of the cavity and the large mass of the mold prevented really rapid quenching of our sample. Also, the annealing time would have to have been orders of magnitude longer in order to approach the homogeneity of Stout and Guttman's samples.

[43] R. A. Ferrell and R. E. Glover, III, Phys. Rev. **109**, 1398 (1958).
[44] F. London, *Superfluids* (John Wiley and Sons, Inc., New York, 1954), Vol. 1.
[45] W. Meissner, H. Franz, and H. Westerhoff, Ann. Physik **13**, 967 (1932).
[46] J. W. Stout and L. Guttman, Phys. Rev. **79**, 396 (1950).

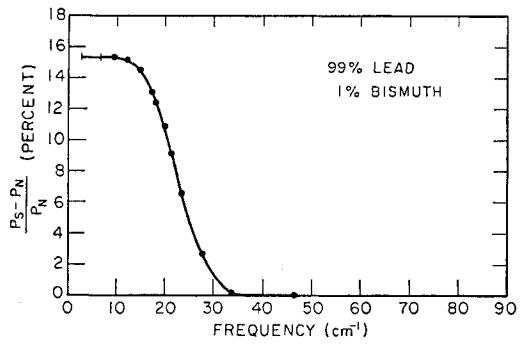

FIG. 13. Absorption curve for cavity made from 99% lead and 1% bismuth.

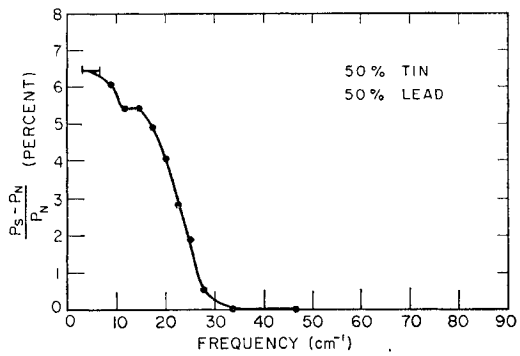

FIG. 14. Absorption curve for cavity made from 50% lead and 50% tin.

A cavity was also made from the two-phase alloy of 50% tin and 50% lead. This mixture separates into badly strained tin-like and lead-like crystal structures as it cools. Figure 14 shows the absorption edge for the tin-lead cavity. It is just a smeared-out average of the tin and lead absorption edges, which start at ~ 9 and ~ 20 cm^{-1}, respectively.

The indistinct gap that we find for superconducting alloys is not inconsistent with the existence of the ordinary superconducting properties such as the Meissner effect, according to the sum rule arguments of Ferrell, Glover, and Tinkham.[3,43] All that these arguments require to predict the properties of the supercurrents at low frequencies is that most of the states be removed from an energy range just above the ground state without any compensating absorption at higher energies. This much is certainly true in our superconducting alloys.

IX. CONCLUSION

We have measured the onset of absorption due to excitation of electrons across the energy gap in a variety of superconductors. Using the onset of the main absorption as a measure of the energy gap, we find the values of $E_g(0)$, the energy gap at absolute zero, to be $4.1\pm0.2\ kT_c$ for indium, $3.6\pm0.2\ kT_c$ for tin, $4.6\pm0.2\ kT_c$ for mercury, $\leqq 3.0\ kT_c$ for tantalum, $3.4\pm0.2\ kT_c$ for vanadium, $4.1\pm0.2\ kT_c$ for lead, and $2.8\pm0.3\ kT_c$ for niobium. The errors given here are estimated limits of experimental error. It is possible, especially in the cases of tantalum and niobium, that the surface layer in which the measurements were made did not have the value of the energy gap characteristic of the pure bulk superconductor. This possibility is not included in our error estimate. Several differently prepared samples of the soft superconductors tin, lead, and mercury did give the same value of the gap.

These values of the energy gap at absolute zero deviate significantly from the BCS value of $3.5\ kT_c$, and the deviation is a fairly smooth function of the Debye temperature alone, but a less smooth one of the ratio of the critical temperature to the Debye temperature. We find generally good agreement between our values of the energy gap and those inferred by other methods, except for tantalum, niobium, and mercury. The disagreement in the case of mercury appears to be significant since we were able to repeat our measurements with different samples.

We find evidence for structure on the absorption curves of lead and mercury. The interpretation of this structure is not certain, but it is probably due to anisotropy of the energy gap, to collective excitations from the superconducting ground state, or to a dielectric anomaly. The evidence at present is not sufficient to finally rule out any of these possibilities, but anisotropy seems the most likely interpretation. The main absorption edge appears to scale with temperature according to the BCS temperature dependence of the energy gap, and the structure appears to shift in a roughly similar manner.

Attempts to fit our absorption edge data to theories of the skin effect in the superconducting and normal states are complicated by the fact that our measurements were not made under conditions leading to any simple limiting case of the theory. It does appear, however, that σ_1/σ_N must rise somewhat more rapidly above the gap than is predicted by the theory of Mattis and Bardeen. The fact that at no frequency do we observe more absorption in the superconducting than in the normal state allows us to place some limitations on the behavior of σ_1/σ_N and σ_2/σ_N beyond the energy gap.

As might be expected from the broad superconducting transitions in most alloys, the absorption edges for alloy cavities are less sharp than for pure superconductors. This indicates that the gap is not sharply defined over-all in most alloy superconductors, though it may be on a microscopic scale.

X. ACKNOWLEDGMENTS

The authors are pleased to acknowledge the assistance of D. M. Ginsberg, who collaborated in the design and construction of the monochromator.